Supplementary material

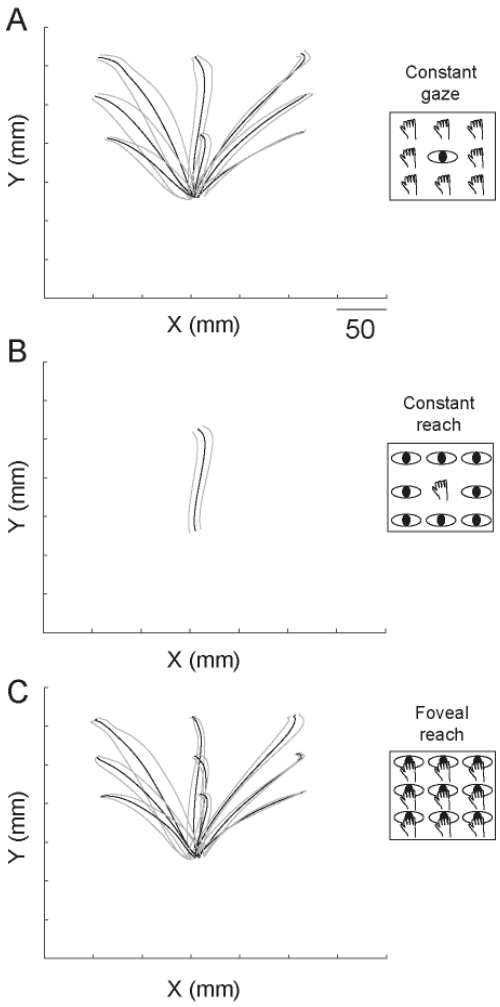

figure S1

Fig. S1

Actual trajectories of the reaching movement in the Sham condition. The trajectories of the index finger during movement in each of the three eye-hand configurations in one participant are shown. Black lines indicate the averaged trajectory and gray lines the X and Y variabilities along the movement.

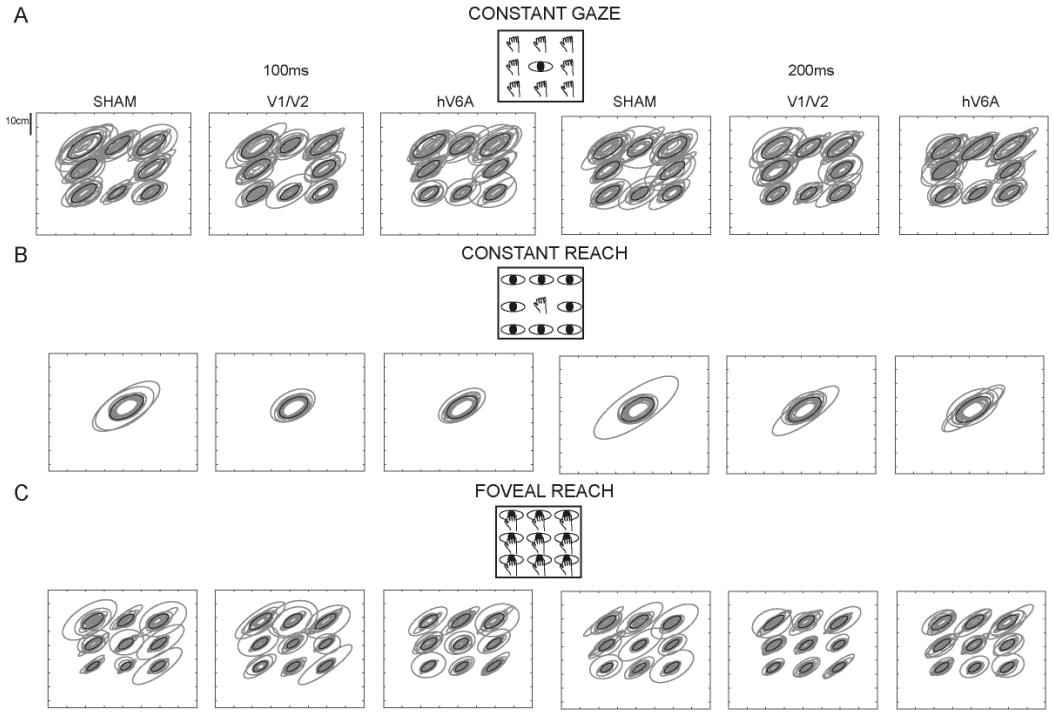

fig. S2

Fig. S2

Reaching precision in the different stimulation conditions.

A-C) Mean endpoint confidence ellipses for all 15 subjects (gray circles) and mean ellipses across all the subjects (black circles) during the visually-guided immediate reaching task in each of the 3 eye-hand configurations (top: Constant gaze; middle: Constant reach; bottom: Foveal reach). in 100-ms trials (left). in 200-ms trials (right). and in each of the 3 stimulation conditions (Sham. left. V1/V2. middle. hV6A. right. respectively). Horizontal and vertical axes correspond to the x- and y-coordinates in the horizontal plane. Despite the huge effects of depth and direction. no effect of spTMS on hV6A were found.

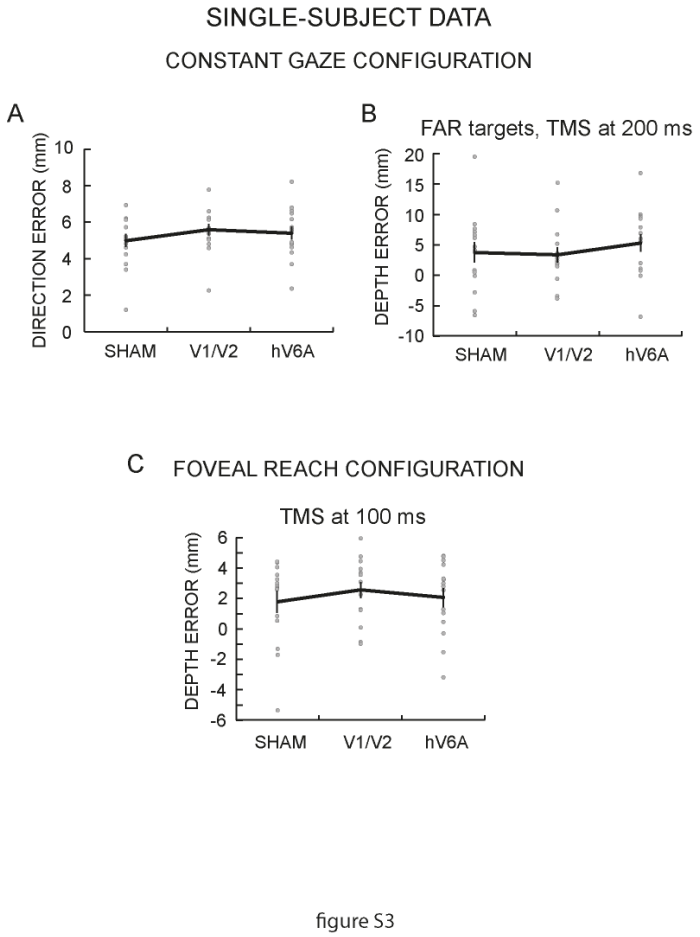

figure S3

Fig. S3

Single subject data

A) Direction errors of single subjects (grey dots) and mean value with SE (black line) in TMS delivered during Sham stimulation (SHAM), V1/V2 stimulation (V1/V2), and hV6A stimulation (hV6A) in the constant gaze configuration. B) Depth errors of single subjects (grey dots) and mean value with SE (black line) in TMS delivered during Sham stimulation (SHAM), V1/V2 stimulation (V1/V2), and hV6A stimulation (hV6A) in the constant gaze configuration for reaching towards far targets and TMS delivered after 200 ms of reaction time. C) Depth errors of single subjects (grey dots) and mean value with SE (black line) in TMS delivered during Sham stimulation (SHAM), V1/V2 stimulation (V1/V2), and hV6A stimulation (hV6A) in the foveal reach configuration with TMS delivered after 100 ms of reaction time.

Reach end-point precision

Constant gaze configuration (peripheral reaching)

Reach end-point precision was measured as the area of 95% confidence ellipses of the scatter of the fingertip at movement end (see Materials and Methods) (Fig. 1E). Figure S2A shows the ellipses of all the subjects (gray). and the mean ellipse (black) for the Constant gaze configuration.

We found that stimulation of hV6A did not influence the end-point precision in the constant gaze configuration (main effect of Stimulation Condition or interaction of the other factors by Stimulation Condition. all $F < 1.65$. all $p > 0.17$. all partial $\eta^2 < 0.1$). in agreement with previous studies of repetitive TMS delivered on the medial parietal cortex (Vesia et al. 2010), namely SPOC (Cavina-Pratesi et al. 2010) and on a more anterior parietal region (Marigold et al. 2019) homologue of monkey areas PEc/PE (Pitzalis et al. 2019).

As evident in the figure, a significant main effect of Depth ($F_{(2.28)} = 30.95$; $p < 0.001$. partial $\eta^2 = 0.69$) was found. Post hoc tests revealed that the precision during reaches towards farthest targets (9.88 mm^2 +/- 1.14) was lower than the one for reaches towards intermediate (6.64 mm^2 +/- 0.76) and near targets (5.65 mm^2 +/ -0.78. all $p < 0.001$. Fig. S2A). which in turn did not differ from one another ($p = 0.09$).

We also found a significant main effect of Direction ($F_{(2.28)} = 32.12$. $p < 0.001$. partial $\eta^2 = 0.69$) with reaches towards intermediate targets (4.46 mm^2 +/ -0.64) having the highest precision (right = 6.71 mm^2 +/- 0.82; left = 7.75 mm^2 +/ -0.9. $p < 0.001$ intermediate vs right and intermediate vs left. $p = 0.02$ right vs left).

Constant reach configuration (peripheral reaching)

A significant effect of Depth on precision was found ($F_{(2.28)} = 10.5$. $p < 0.001$. partial $\eta^2 = 0.42$): when gaze directed towards near targets (7.56 mm^2 +/- 0.77), reach was less precise than in the other configurations (far = 5.44mm^2 +/- 0.82; intermediate = 5.93 mm^2 +/- 0.68. near vs far and near vs intermediate $p = 0.002$; far vs intermediate $p = 0.32$).

We also found a significant main effect of Direction ($F_{(2.28)} = 33.2$. $p < 0.001$. partial $\eta^2 = 0.70$) with reaches towards central targets (4.01 mm^2 +/- 0.54) showing the highest precision (right = 9.10mm^2 +/- 1.08; left = 6.99 mm^2 +/- 1.05. $p < 0.001$ center vs right and center vs left. $p = 0.002$ right vs left).

Foveal reach configuration (foveal reaching)

A significant main effect of Depth (Figure S2C. $F_{(2.28)} = 12.4$. $p < 0.001$. partial $\eta^2 = 0.47$) was found. Similarly to the Constant gaze configuration. precision during foveal reaching towards farthest targets (4.67 mm^2 +/- 1.15) was lower than the one for reaching towards intermediate (2.69 mm^2 +/- 0.56) and near targets (2.35 mm^2 +/- 0.56. $p < 0.001$), which in turn did not differ from one another ($p = 0.49$).

No significant effects of Direction were found . all $F < 0.82$. all $p > 0.24$. all partial $\eta^2 < 0.09$.

Table S1

Mean values and standard errors of the reaction time and movement time of participants in different stimulation conditions (S = sham. hV6A = hV6A. V1/V2 = V1/V2). at different times (100ms. 200ms) and at different target depths (F = far. I = intermediate. N = near) of the Constant gaze configuration. RT = reaction time; MT = movement time; SE = Standard Error.

Stimulation condition	Stimulation Time	Depth	RT mean (ms)	RT SE	MT mean (ms)	MT SE
S	100	F	414.13	21.61	837.74	74.12
S	100	I	429.83	31.61	719.64	60.17
S	100	N	385.75	20.21	647.57	60.76
S	200	F	420.01	20.04	844.40	73.10
S	200	I	419.24	24.51	733.72	60.76
S	200	N	391.83	19.40	633.55	52.20
V1/V2	100	F	396.11	19.89	824.83	63.36
V1/V2	100	I	398.82	23.49	727.37	62.40
V1/V2	100	N	389.72	25.31	618.77	45.26
V1/V2	200	F	413.41	19.81	827.25	67.14
V1/V2	200	I	407.07	19.68	731.16	61.50
V1/V2	200	N	398.12	21.83	618.54	48.83
hV6A	100	F	432.11	33.80	840.52	67.56
hV6A	100	I	410.29	25.09	732.69	59.65
hV6A	100	N	384.38	20.82	626.34	45.43
hV6A	200	F	424.24	20.53	815.46	65.70
hV6A	200	I	424.12	24.12	726.36	56.78
hV6A	200	N	389.02	19.50	629.74	46.88

References

Cavina-Pratesi C. Monaco S. Fattori P. Galletti C. McAdam TD. Quinlan DJ. Goodale MA. Culham JC. 2010. Functional magnetic resonance imaging reveals the neural substrates of arm transport and grip formation in reach-to-grasp actions in humans. J Neurosci. 30:10306–10323.

Marigold DS. Lajoie K. Heed T. 2019. No effect of triple-pulse TMS medial to intraparietal sulcus on online correction for target perturbations during goal-directed hand and foot reaches. PLoS One. 14:e0223986.

Pitzalis S. Serra C. Sulpizio V. Di Marco S. Fattori P. Galati G. Galletti C. 2019. A putative human homologue of the macaque area PEc. Neuroimage.

Vesia M. Prime SL. Yan X. Sergio LE. Crawford JD. 2010. Specificity of human parietal saccade and reach regions during transcranial magnetic stimulation. J Neurosci. 30:13053–13065.